MedCrave
Step into the World of Research

Journal of Nanomedicine Research

Research Article

Open Access

CrossMark

# Synthesis and thermal behavior of nanopowders in $LaPO_4$-$YPO_4$(-$H_2O$), $LaPO_4$-$LuPO_4$(-$H_2O$) and $YPO_4$-$ScPO_4$(-$H_2O$) systems for ceramic matrices

## Abstract

Nanosized powders in the $LaPO_4$-$YPO_4$(-$H_2O$), $LaPO_4$-$LuPO_4$(-$H_2O$) and $YPO_4$-$ScPO_4$(-$H_2O$) systems have been synthesized to increase the mutual solubility of initial components and to prepare effective ceramic matrices by sintering them. Ceramic matrices were characterized by high isomorphic capacity, thermal and chemical resistance.

**Keywords:** Sol-gel,Ln'1–xLn"xPO4·$nH_2$ nanopowders, Ceramic matrices, Thermal, Chemical stability

Volume 6 Issue 1 - 2017

Larisa Mezentseva,[1] Alexandr Osipov,[1] Valery Ugolkov,[1] Andrey Akatov,[2] Valery Doilnitsyn,[2] Tatiana Maslennikova,[1] Aleksandr Yakovlev[3]

[1]Grebenshchikov Institute of Silicate Chemistry, Russian Academy of Sciences, Russia

[2]Saint-Petersburg State Institute of Technology (Technical University), Russia

[3]ITMO University, Russia

**Correspondence:** Larisa Mezentseva, Grebenshchikov Institute of Silicate Chemistry, Russian Academy of Sciences, Makarova emb., 2, Saint-Petersburg, 199034, Russia, Tel 7 (812)325-41-36, Fax 7 (812)328-85-89, Email la_mez@mail.ru

**Received:** July 05, 2017 | **Published:** August 18, 2017

## Introduction

In many previous works, the monazite-type lanthanum orthophosphate (LaPO4), and xenotime one (YPO4) has been suggested as matrices for radioactive waste immobilization (radioactive rare earth elements or trivalent actinides) and sensors.[1-8] Nanopowder-based ceramics designed for immobilizing purpose should possess high chemical resistance and isomorphic capacity, high durability and thermal stability. It is supposed to use ceramics obtained by sintering nanopowders with general formula Ln'1–xLn"xPO4 $nH_2$ synthesized by sol-gel technique with inverse precipitation and further dehydrated upon high heating rate to retain nanoscale. From this point of view the aim of this study was to investigate peculiarities of formation of nanopowders in the systems where components belong to the same or different structural groups, to determine their isomorphic capacity, to study thermal behavior, and thereby to develop physical and chemical approaches to prepare ceramic samples (as matrices) based on them. In this case the second component plays a role of immobilized ion (isotope).

The hydrated La orthophosphate crystallizes in hexagonal rhabdophane-type system upon precipitation and contain 0.5-3 moles of $H_2$ per formula unit. At temperature higher than 600 °C nanosized crystals loose water molecules and transform into monoclinic monazite-type form.[9] Yttrium, lutetium and scandium orthophosphates, hydrated and dehydrated, crystallizes in tetragonal xenotime-type form.[9,10] In this instance it was expected formation of limited solid solutions in the $LaPO_4$-$YPO_4$(-$H_2O$) and $LaPO_4$-$LuPO_4$(-$H_2O$) systems[9] and unlimited solid solutions in the $YPO_4$-$ScPO_4$(-$H_2O$) system.[10]

Hydrated rare earth orthophosphate nanopowders were synthesized using sol-gel method at stoichiometric ratio of interacting components $Ln(NO_3)$

3 and $NH_4H_2PO_4$ in an aqueous solution in the form of stable colloids that coagulate at pH ≈ 7.[9-11] The use of reverse precipitation as it was shown allows improving further physico-mechanical properties of ceramic samples (matrices) obtained by sintering of nanopowders preliminary calcined to remove water from crystalline lattice.[10,11]

## Experimental

The initial reagents for rare earth orthophosphate systems were REE2O3 (special-purity grade, 99.999%), mono substituted ammonium phosphate (special-purity grade, 99.5%), nitric acid (special-purity grade, 70%), aqua ammonia (special-purity grade, 25%), and distilled water. Synthesis of Ln'1–xLn"xPO4 $nH_2$ nanopowders was performed by sol-gel technique according the reactions described.[11]

The proper pH ≈ 7 for complete precipitation was reached by NH4OH addition. The precipitates were kept in the mother liquor for 24 h, washed after that by decantation, filtered off, and air-dried at 110 °C for 24 h.[9,11] For X-ray powder diffraction analysis DRON-3 diffractometer (Russia) was used. Recording parameters were as follows: Ni-filtered Cu$K\alpha$ radiation, 38 kV, time constant 1, scanning speed 1 degree per minute. The thermal behavior of the samples was studied by means of stepwise heating of powders compacted into tablets under a pressure of 8–10 MPa within the temperature range of 850–1700 °C with further analysis by XRD or differential scanning calorimetry (DSC) and thermal gravimetry (TG).

The DSC/TG measurements were conducted in STA 449C (NETZSCH) calorimeter; sample mass was about 30 mg; heating rate was 20 °C/min. Preliminary calcined at 850 °C for 2 h nanopowders *were* compacted into tablets under a pressure of 8-10 MPa and then stepwise heated in air at 1000, 1200, 1600 and 1700 °C to obtain ceramic samples (matrices). Vickers microhardness measurement of ceramic samples (matrices) was performed under the loading of 20 g (2 N) using a PMT 3 microhardness meter (Russia) equipped with Microanalysis Microhardness software package developed at JSC LOMO (Russia). Scanning electron microscopy (SEM) was used for powders observations (Tescan Vega 3, Czech Republic).

For leaching experiments, the powders were compacted into cubes with a volume of 1 cm3 under a pressure of 8–10 MPa, after which they were stepwise calcined at 1000 (24 h), 1200 (24 h), and 1600°C (1 h). Ceramic cubes were placed into plastic containers and poured with 50 mL of contact solution (distilled water or 10% HNO3 aqueous solution). The test temperature was 25±3 °C; a contact solution was changed within 1, 3, 7, 10 and 14 days. The La3+ and Y3+ concentrations in the solution upon leaching were determined by inductively coupled plasma mass spectrometry (ICP-MS). ICP-MS test was performed at A.P. Karpinsky Russian Geological Research Institute (St.-Petersburg).

## Results and discussion

Ln'1–xLn"xPO4 $nH_2$ (Ln' = La, Y; Ln" = Y, Sc; $x$ = 0.0-1.0) nanopowders were synthesized by technique described above. According to results of electron microscopy analysis, the powders consist of large agglomerates of nanoscaled particles (Figure 1). The XRD powder patterns of the Ln'1–xLn"xPO4 $nH_2$ are presented in Figure 2-4. They exhibit formation of limited solid solutions at temperature of synthesis (room temperature) for $LaPO_4$-$YPO_4$-$H_2O$ and $LaPO_4$-$LuPO_4$(-$H_2O$) systems and unlimited solid solutions for the $YPO_4$-$ScPO_4$(-$H_2O$) system. Substitutional solid solutions based on hexagonal LaPO4·$nH_2$ extended to $x \approx 0.6$ for Y3+ and Lu3+ (Figure 1-5). Solid solutions based on tetragonal form were observed within narrower concentration range (Figure 2,3,6-9). Due to very broad reflexes precise determent of reflexes belonging to tetragonal solid solutions were difficult.

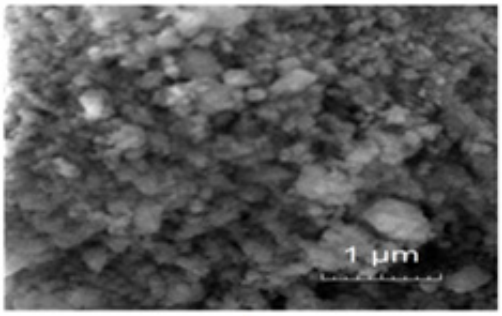


a)

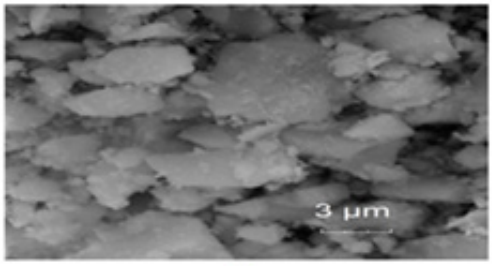


b)

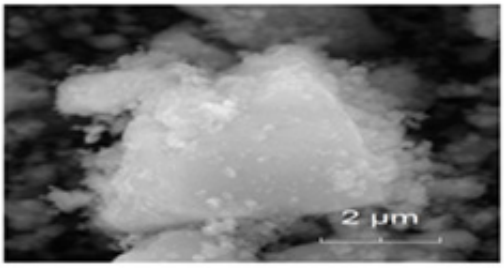


c)

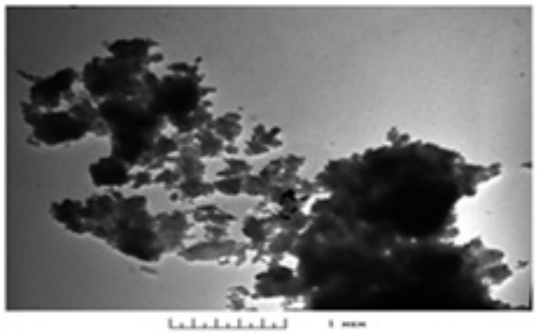

d)

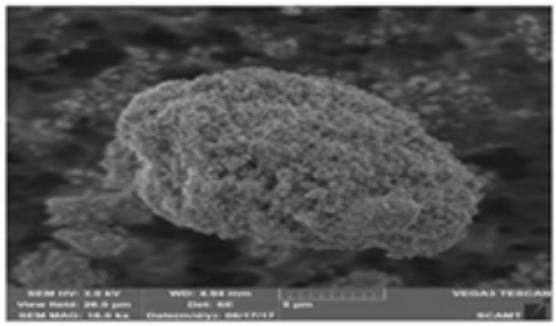

e)

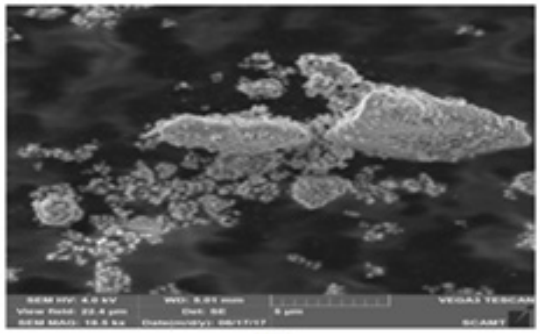

f)

**Figure 1** SEM micrographs: (a) LaPO4•$nH_2$; (b) La0.5Y0.5PO4•$nH_2$; (c) YPO4•$nH_2$; (d) Y0.2Sc0.8PO4•$nH_2$; and electron micrographs: (e) La0.6Lu0.4PO4•$nH_2$; (f) La0.6Lu0.4PO4•$nH_2$ of nanopowders synthesized by reverse (a-d) and direct (e, f precipitation).

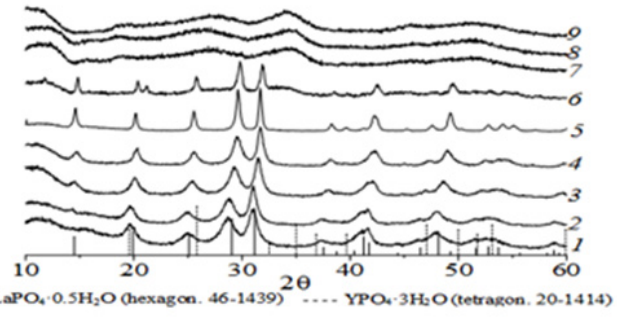


**Figure 2** XRD patterns of initial La1–xYxPO4•$nH_2$ powders (reverse precipitation), for x: 0.0 (1), 0.1 (2), 0.3 (3), 0.5 (4), 0.7 (5), 0.8 (6), 0.9 (7), 0.95 (8), 1 (9), and the bar graphs represent the XRD patterns of LaPO4•0.5$H_2$ and YPO4•3$H_2$ of ICDD-PDF.

**Citation:** Mezentseva L, Osipov A, Ugolkov V, et al. Synthesis and thermal behavior of nanopowders in LaPO4-$YPO_4$(-$H_2O$), $LaPO_4$-$LuPO_4$(-$H_2O$) and $YPO_4$-$ScPO_4$(-$H_2O$) systems for ceramic matrices. *J Nanomed Res.* 2017;6(1):1–6. DOI: 10.15406/jnmr.2017.06.00145

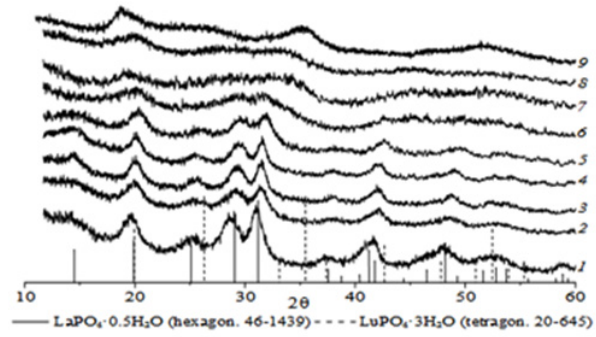


**Figure 3** XRD patterns of initial La1–xLuxPO4•$nH_2$ powders (direct precipitation), for x: 0.0 (1), 0.25 (2), 0.3 (3), 0.4 (4), 0.5 (5), 0.6 (6), 0.7 (7), 0.75 (8), 1.0 (9), and the bar graphs represent the XRD patterns of LaPO4•0.5$H_2$ and LuPO4•3$H_2$ of ICDD-PDF.

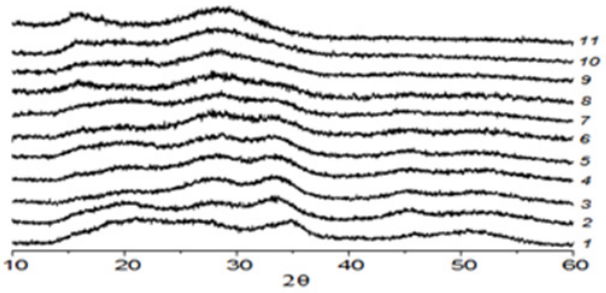


**Figure 4** XRD patterns of initial Y1–xScxPO4·$nH_2$ powders (reverse precipitation), for x: 0.0 (1), 0.1 (2), 0.2 (3), 0.3 (4), 0.4 (5), 0.5 (6), 0.6 (7), 0.7 (8), 0.8 (9), 0.9 (10), 1.0 (11), and the bar graphs represent the XRD pattern of YPO4•3$H_2$ of ICDD-PDF.

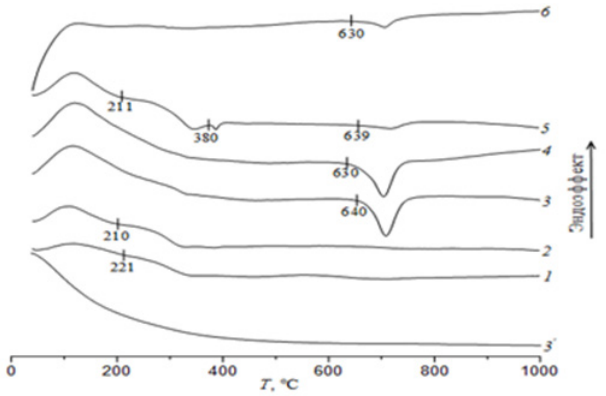


**Figure 5** DSC curves for the La1–xYxPO4•$nH_2$ samples (reverse precipitation), for x: 0.0 (1), 0.3 (2), 0.8 (3), 0.9 (4), 0.95 (5), 1.0 (6). TG curve for La0.2Y0.8PO4•$nH_2$ (3').

Unlimited tetragonal solid solutions formed in the $YPO_4$-$ScPO_4$(-$H_2O$) system in the whole concentration range (Figure 4). According to the DSC/TG results (Figure 5-7), Ln'1–xLn"xPO4 *n*$H_2$ samples loose water in temperature range 50–600 °C and then were stable until at least 1000 °C.

A series of exothermic effects observed at temperatures higher than 600 ºC (single and double) and not accompanied by the mass loss could be referred in our opinion to intensive crystallization of high dispersion powders containing tetragonal almost amorphous phase (Figure 5, curves *3–6*; Figure 6, curves 1–10). Isomorphic capacity of dehydrated monoclinic LaPO4 herewith appeared to be less then 80 mol% of YPO4 (Figure 5, curve *3*). Before sintering, Ln'1–xLn"xPO4 *n*$H_2$ powders were calcined at temperature not higher then 850 °C (1 or 2 h) to keep high dispersion of dehydrated samples.[12,13] These anhydrous Ln'1–xLn"xPO4 powders were then pressed into tablets and stepwise heated up to 1600-1700 °C to obtain ceramic samples (matrices).

Fracture surfaces of La1–*x*Y*x*PO4 ceramic samples (matrices) calcined at different temperatures are presented in Figure 7. Here well created roundish grains which size does not exceed 2-3 μ are observed. Determined open porosity of ceramic samples is low and is in the range of 0.1-0.2%.[12]

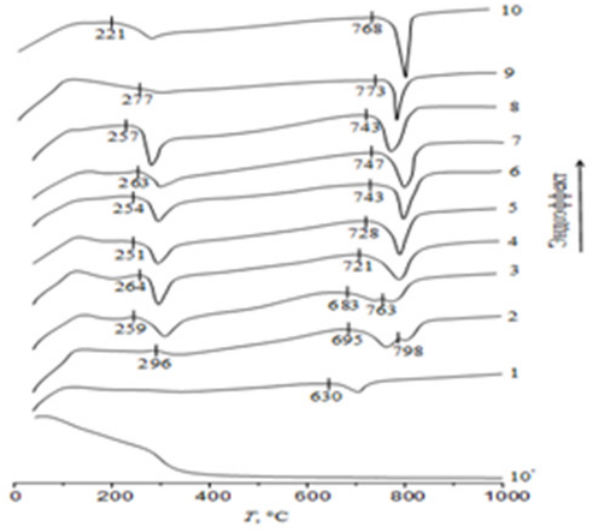


**Figure 6** DSC curves for the Y1–xScxPO4·$nH_2$ samples (reverse precipitation) for x: 0.0 (1), 0.2 (2), 0.3 (3), 0.4 (4), 0.5 (5), 0.6 (6), 0.7 (7), 0.8 (8); 0.9 (9), 1.0 (10). TG curve for ScPO4•$nH_2$ (10').

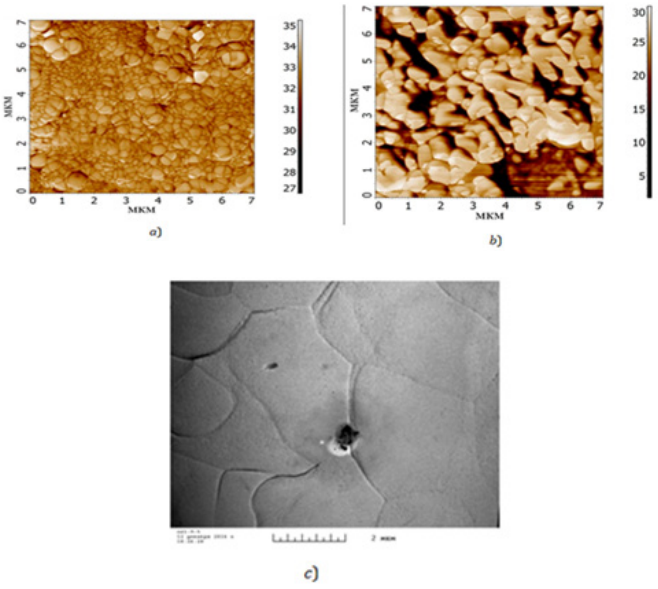


**Figure 7** Fracture surface of La0.5Y0.5PO4 ceramic sample (matrix) calcined at 1000 °C for 24 h (a), 1200 °C for 24 h (b), NTEGRA atomic-force microscope; 1700 °C for 1 h (c), EM transmission electron microscope; black spots are remains of zylonite (celluloid) replica.

**Citation:** Mezentseva L, Osipov A, Ugolkov V, et al. Synthesis and thermal behavior of nanopowders in $LaPO^4$-$YPO_4$(-$H_2O$), $LaPO_4$-$LuPO_4$(-$H_2O$) and $YPO_4$-$ScPO_4$(-$H_2O$) systems for ceramic matrices. *J Nanomed Res.* 2017;6(1):1–6. DOI: 10.15406/jnmr.2017.06.00145

According to calculated lattice parameters for monoclinic La1–*x*Y*x*PO4 and La1–*x*Lu*x*PO4 series calcined at 1000 °C, 24 h isomorphic capability was about 70 mol% for YPO4 and 20-25 mol% for LuPO4.[9,12] It is worth to compare the values with isomorphic capacity of monoclinic LaPO4 in respect of HoPO4 (~30 mol%)[13] which is in a good accordance with ionic radii for coordination number 8 (Y3+ 0.116; Ho3+ 0.115; Lu3+ 0.112 nm).

The microhardness values of Ln'1–xLn"xPO4 ceramic samples (matrices) calcined at different temperatures are given in Table 1. These values depend on the chemical composition, a ratio of components and heat treatment temperature. They are significantly higher than those obtained for individual La, Gd, Dy or Y phosphate ceramics (4.5-7.8 GPa)[14-18] or 7.2 GPa for phosphate glass ceramics, and 8.0–8.5 GPa for SYNROC.[19] This could be associated with very high dispersion of initial powders. Leaching experiments exhibit quite good resistance of Ln'1–xLn"xPO4 matrices in a strongly acid HNO3 solution (pH 1-2) at room temperature (Figure 8 & 9). The results of leaching experiments for Ln'1–xLn"xPO4 are close to[20] for GdPO4 in strongly HCl and HNO3 solutions (pH 1–2) corresponding to value of ~10–2 g L–1.

**Table 1** Microhardness for La1–xYxPO4 and Y1–xScxPO4 ceramic samples (matrices) after heat treatment

| Состав образца | Microhardness, GPa, ± 0.1 | | | |
|---|---|---|---|---|
| | Heat Treatment Temperature, °C | | | |
| | 1000 (24 h) | 1200 (24 h) | 1600 (1 h) | 1700 (1 h) |
| $LaPO_4$ | 10.7 | 23.9 | – | – |
| $La_{0.9}Y_{0.1}PO_4$ | 10.9 | 24.9 | 26.5 | – |
| $La_{0.7}Y_{0.3}PO_4$ | 18.7 | 21 | 24.2 | – |
| $La_{0.5}Y_{0.5}PO_4$ | 10.5 | 18.8 | – | – |
| $La_{0.3}Y_{0.7}PO_4$ | 9.3 | 17.3 | – | – |
| $La_{0.2}Y_{0.8}PO_4$ | 10.2 | 19.7 | 22.5 | – |
| $La_{0.1}Y_{0.9}PO_4$ | 13.5 | 22.6 | – | – |
| $La_{0.05}Y_{0.95}PO_4$ | 12.1 | 21.4 | – | – |
| $YPO_4$ | 11 | 17.7 | 22.1 | 27.9 |
| $YPO_4$ | 11 | 17.7 | 22.1 | 27.9 |
| $Y_{0.9}Sc_{0.1}PO_4$ | 8.5 | 17.9 | 21.7 | 27 |
| $Y_{0.8}Sc_{0.2}PO_4$ | 8.1 | 17.4 | 20.1 | 26.6 |
| $Y_{0.7}Sc_{0.3}PO_4$ | 7.8 | 16.9 | 19.2 | 24.1 |
| $Y_{0.6}Sc_{0.4}PO_4$ | 7.3 | 16.3 | 19.1 | 24.5 |
| $Y_{0.5}Sc_{0.5}PO_4$ | 7.4 | 15.4 | 18.4 | 23.6 |
| $Y_{0.4}Sc_{0.6}PO_4$ | 7.2 | 14.5 | 18 | 23.8 |
| $Y_{0.3}Sc_{0.7}PO_4$ | 6.8 | 13.4 | 17.7 | 23.2 |
| $Y_{0.2}Sc_{0.8}PO_4$ | 6.9 | 12.7 | 16.9 | 22 |
| $Y_{0.1}Sc_{0.9}PO_4$ | 6.5 | 11.9 | 16.5 | 22.7 |
| $ScPO_4$ | 5.8 | 11.5 | 15.8 | 21.3 |

Leaching rate of both ions for La1–xYxPO4 is within the range 10–3-10–2 g/(cm2 day) that is lower than the leaching rate in distilled water for La3+ and Y3+ ions (10–6-10–7 g/(cm2 day))[13] but compared with leaching rate of Y3+ for Y1–xScxPO4 (10–5-10–7 g/(cm2 day)) presented in Figure 9. It is worth to note that for La1–xYxPO4 matrices almost no falling of rate is observed. Usually at first the ceramic cube surface is intensively dissolved, and then rate decreases, being limited to diffusion. It looks like a uniform etching. In this case Y1–xScxPO4 matrices are considered as a very steady system.

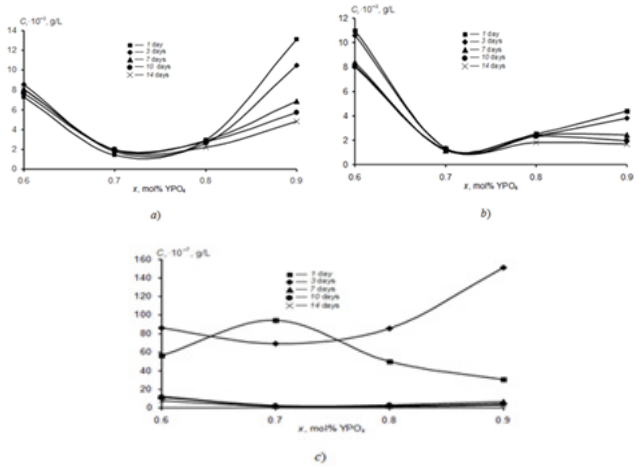

**Figure 8** Ions concentration (C) in contact solutions (10% HNO3) during leaching experiments: a) La3+ for La1–xYxPO4 matrices; b) Y3+ for La1–xYxPO4 matrices; c) Y3+ for Sc1–xYxPO4 matrices.

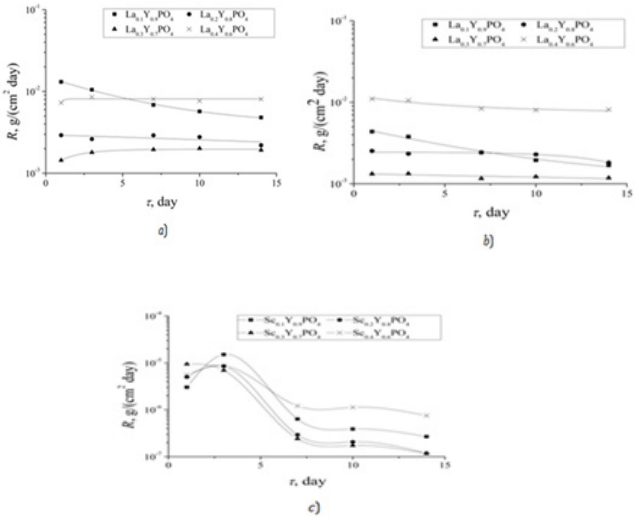

**Figure 9** Dependence of leaching rate (R) of La3+ (a) and Y3+ (b, c) ions on duration of leaching (τ) in HNO3 contact solutions (10%) for La1–xYxPO4 (a, b) and for Sc1–xYxPO4 (c) ceramic matrices.

## Summary

High dispersion La1–xYxPO4·$nH_2$ and Y1–xScxPO4·$nH_2$ powders were synthesized by sol-gel technique with reverse precipitation, and La1–xLuxPO4·$nH_2$ powders with direct precipitation.

Ln'1–xLn"xPO4 ceramic samples (matrices) obtained by sintering of preliminary dehydrated powders exhibited high isomorphic capacity in respect of the second components playing role of an immobilized ion (isotope), i.e. up to 70 mol% of YPO4, 20-25 mol% of LuPO4 and complete mutual solubility in Y1–xScxPO4·series.

Ln'1–xLn"xPO4 ceramic samples (matrices) were stable up to 1600(1700) ºC, and possessed high microhardness increased with increasing heat treatment temperature (up to 28 GPa). Leaching rate of both lanthanum and yttrium ions from La1–xYxPO4 ceramic matrices was almost within the range 10–3-10–2 g/(cm2 day), and yttrium ions from Y1–xScxPO4 ceramic matrices were lower (within the range 10–5-10–7 g/(cm2 day)). Therefore, rare earths orthophosphate ceramic matrices are suitable to immobilize radioactive waste relating to actinide/rare-earth group occurred in high level waste (HLW)

**Citation:** Mezentseva L, Osipov A, Ugolkov V, et al. Synthesis and thermal behavior of nanopowders in $LaPO^4$-$YPO_4(-H_2O)$, $LaPO_4$-$LuPO_4(-H_2O)$ and $YPO_4$-$ScPO_4(-H_2O)$ systems for ceramic matrices. *J Nanomed Res.* 2017;6(1):1–6. DOI: 10.15406/jnmr.2017.06.00145

because they possess high chemical resistance, isomorphic capacity, thermal stability and microhardness.

## Acknowledgments

The authors gratefully acknowledge the financial support of this work by the Russian Foundation for Basic Research, project no. 15-03-04020-a.

## Conflicts of interest

None.

## References

1. Terra O, Clavier N, Dacheux N, et al. Preparation and characterization of lanthanum–gadolinium monazites as ceramics for radioactive waste storage. *New J Chem*. 2003;27(6):957–967.
2. Volkov YuF. Compounds with zircon and monazite structures and possibilities of their use for incorporation of radionuclides. *Radiochemistry*. 1999;41(2):168–174.
3. Picot V, Deschanels X, Peuget S, et al. Ion Beam Radiation Effects in Monazite. *J Nucl Mater*. 2008;381(3):290–296.
4. Wang L, Liang T. Ceramics for high level radioactive waste solidification. *J Adv Ceram*. 2012;1(3):194–203.
5. Schlenz H, Heuser J, Neumann A, et al. Monazite as a Suitable Actinide Waste Form. *Z Kristallogr (Cryst Mater)*. 2013;228(3):113–123.
6. Moses WW, Weber MJ, Derenzo SE, et al. Prospects for dense, infrared emitting scintillators. *IEEE Trans Nucl Sci NS*. 1998;45(3):462–466.
7. Di W, Shirahata N, Zeng H, et al. Fluorescent sensing of colloidal CePO4: Tb nanorods for rapid, ultrasensitive and selective detection of vitamin C. *Nanotechnology*. 2010;21(36):365501.
8. Lv C, Di W, Liu Z, et al. Luminescent CePO4: Tb colloids for $H_2$2 and glucose sensing. *Analyst*. 2014;139(18):4547–4555.
9. Mezentseva L, Osipov A, Ugolkov V, et al. Solid solutions and thermal transformations in the nanosized LaPO4–YPO4–$H_2$ and LaPO4–LuPO4–$H_2$ systems. *J Ceram Sci Tech*. 2014;5(3):237–244.
10. Mezentseva LP, Osipov AV, Ugolkov VL, et al. Synthesis and physicochemical analysis of powders in the YPO4–ScPO4–$H_2$ system. Modern Tendencies in the Development of Science and Technology, Proc of the VIII International Theoretical and Practical Conference, Advanced Scientific Research Agency (APNI), Russia, 2015;p.14–18.
11. Mezentseva LP, Kruchinina IYu, Osipov AV, et al. Physical–chemical properties of nanopowders and ceramic samples of REE orthophosphates. *Glass Phys Chem*. 2017;43(1):98–105.
12. Mezentseva LP, Kruchinina IYu, Osipov AV, et al. Nanopowders of orthophosphate LaPO4–YPO4–$H_2$ system and ceramics based on them. *Glass Phys Chem*. 2014;40(3):356–361.
13. Ugolkov VL, Mezentseva LP, Osipov AV, et al. Synthesis of nanopowders and physicochemical properties of ceramic matrices of the LaPO4–YPO4–($H_2$) and LaPO4–HoPO4–($H_2$) systems. *Russ J Appl Chem*. 2017;90(1):28–33.
14. Wang R, Pan W, Chen J, et al. Synthesis and sintering of LaPO4 powder and its application. *Mater Chem Phys*. 2003;79(1):30–36.
15. Hay RS, Boakye EE, Mogilevsky P. Transformation plasticity in TbPO4 and (Gd,Dy)PO4 orthophosphates during indentation of polycrystalline specimens. *J Europ Ceram Soc*. 2014;34(3):773–781.
16. Min W, Miyahara D, Yokoi K, et al. Thermal and mechanical properties of sintered LaPO4–Al2O3 composites. *Mater Res Bull*. 2001;36(5–6):939–945.
17. Wang R, Pan W, Chen J, et al. Properties and microstructure of machinable Al2O3/LaPO4 ceramic composites. *Ceram Int*. 2003;29(1):19–25.
18. Kuo DH, Kriven WM. Characterization of yttrium phosphate and yttrium phosphate/yttrium aluminate laminate. *J Am Ceram Soc*. 1995;78(11):3121–3124.
19. Ojovan MI, Lee WE. An Introduction to Nuclear Waste Immobilisation. (2nd edn), Elsevier, Netherlands, 2014;pp.283–305.
20. Glorieux B, Matecki M, Fayon F, Coutures JP, Palau S, et al. (2004) Study of lanthanum orthophosphates polymorphism, in view of actinide conditioning. J Nucl Mater 326(2-3): 156-162.